Wear 265 (2008) 1087–1092

Contents lists available at ScienceDirect

Wear

journal homepage: www.elsevier.com/locate/wear

Sliding wear behavior of copper–graphite composite material for use in maglev transportation system

X.C. Ma[a,b], G.Q. He[a,b,*], D.H. He[c], C.S. Chen[a,b], Z.F. Hu[a,b]

[a] School of Materials Science and Engineering, Tongji University, Shanghai 200092, PR China
[b] Shanghai Key Laboratory for R&D and Application of Metallic Functional Materials, Tongji University, Shanghai 200092, PR China
[c] National Maglev Transportation Engineering R&D Center, Shanghai 201204, PR China

ARTICLE INFO

Article history:
Received 21 August 2007
Received in revised form 4 February 2008
Accepted 19 February 2008
Available online 9 April 2008

Keywords:
Contact material
Metallic composite
Sliding wear
Electric wear
Maglev vehicle

ABSTRACT

This paper reports the study of sliding wear behavior of a copper–graphite composite material (CGCM) for use in maglev vehicles and high-speed railway trains, prepared by means of the powder metallurgy method. The investigated samples were formed by cold pressing at 300 MPa, followed by sintering (950 °C × 3 h) in a hydrogen atmosphere. After specimens were cooled to room temperature with the furnace, a second pressing was performed at 300 MPa. Wear tests were conducted under laboratory conditions with a specially designed sliding wear apparatus, which simulated the tribological conditions of sliding current collectors in a maglev system. The material was slid against a stainless steel band under unlubricated conditions. Worn surfaces of the material were analyzed by scanning electron microscopy (SEM) and field-emission-gun environment SEM (ESEM) equipped with an energy dispersive X-ray spectroscopy (EDS). Within the studied range of normal pressure and electrical current, the wear loss increased with the increasing normal pressure and electrical current. Adhesive wear, abrasive wear and arc erosion were the dominant mechanisms during the electrical sliding. It provides a better understanding principle of design suitable sliding counter parts for the current collection device in maglev systems.

1. Introduction

With the technology developments of electric railways and the maglev system, speedup of trains and cost reduction of maintenance facilities are strongly required [1–6]. Major efforts have been devoted to solving these issues and to meeting the expectations. The collector is one of the factors, which can greatly affect the speedup of vehicle and the cost of maintenance.

It is true that maglev vehicle do have the period of touch power rail during operation. Normally, maglev vehicle running (500 km/h speed) using the power of on board battery, but have to use the power of power rail when runs into the station and some special designed parking area. The design of maglev transportation system is used the power generating coils on top of suspension magnet during high speed, but loss the efficiency of power generating due to lower speed. Therefore, the maglev vehicle also needs a suitable power collecting system to maintain the on board battery power while running at low speed (under 100 km/h speed). Fig. 1 has shown a working scheme of maglev transportation system, where the power rail (10) is parallel to the guideway (2) with mounted on the insulator. The collector (11) is hidden in side of suspension magnet unit (5), and slides on the top of power rail (10) to collect power.

Copper–graphite composite material (CGCM) is a promising contact material for high-speed electrified railways and maglev system, which has an excellent combination of mechanical strength and electrical conductivity [2,6]. Using a simple powder metallurgy (P/M) route for its manufacture, the material is based on the concept of the combined properties of a copper matrix for good electrical conduction and self-lubricant storage (pores) for good wear performance.

The wear behavior between the contact material and the power rail in power collection systems represents a complex tribological system [7–11]. Therefore, a better understanding of the electrical sliding wear behavior of the collector is required for better collecting device design purposes. In this work, a specially built sliding wear tester was used, with a contact strip slid against a stainless steel band, and the sliding wear behavior was studied under power of maglev vehicle required. The wear mechanism of the counterparts is discussed.

* Corresponding author at: School of Materials Science and Engineering, Tongji University, Shanghai 200092, PR China. Tel.: +86 21 65982463; fax: +86 21 65983462.
E-mail address: gqhe@mail.tongji.edu.cn (G.Q. He).

0043-1648/$ – see front matter © 2008 Elsevier B.V. All rights reserved.
doi:10.1016/j.wear.2008.02.015

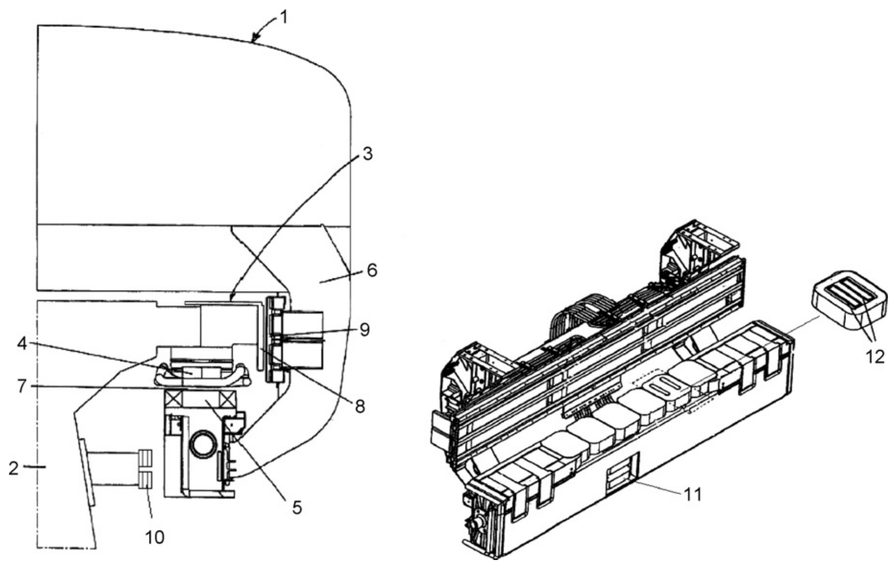

Fig. 1. Schematic drawing of the maglev system (copy from PCT/DE2005/000406). (1) Vehicle body; (2) guideway; (3) sliding surface; (4) longstator; (5) suspension magnet; (6) suspension frame; (7) longstator winding cable; (8) guiding surface; (9) guiding magnet; (10) power rail; (11) current collector; (12) power generating coiler.

2. Experimental procedure

2.1. Specimen

2.1.1. Preparation

The samples used for this study are made by powder metallurgy, which the process included mixing, compacting, sintering and re-pressing. For mixing, a conventional laboratory powder mixer was used. The mixing time was 12 h. The components were initially compacted at cold state in a special designed die at the pressure of 300 MPa. Sintering was carried out at the temperature of 950 °C in hydrogen atmosphere for 3 h. After the specimens cooled to room temperature under protective atmosphere, a second pressing was performed at 300 MPa.

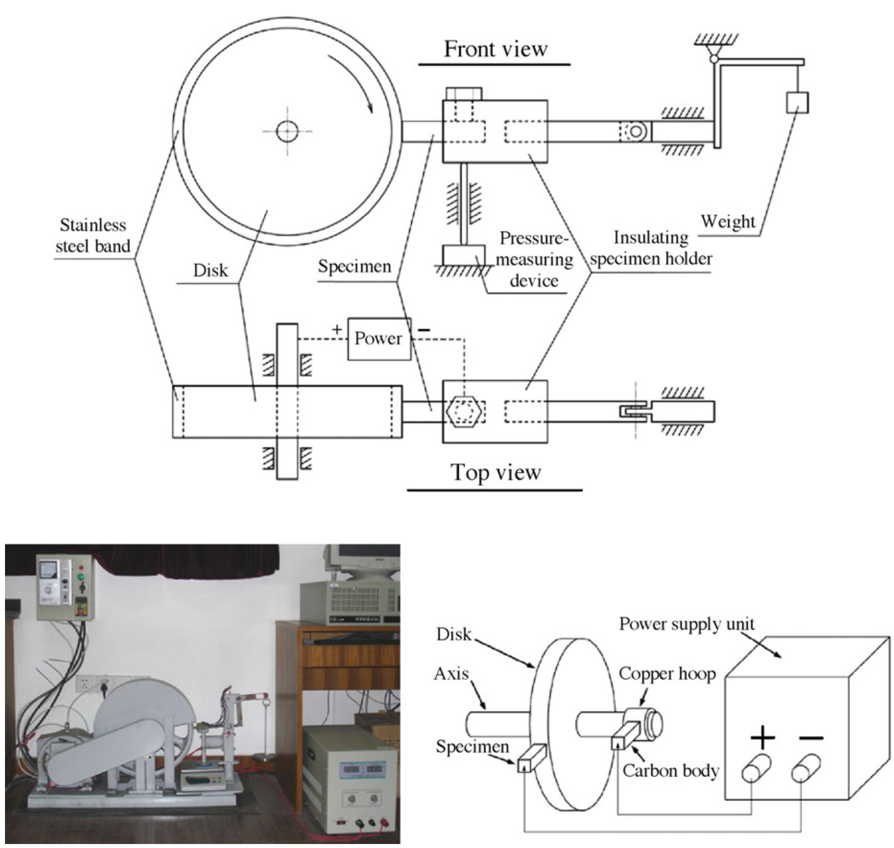

Fig. 2. Schematic of the test apparatus.

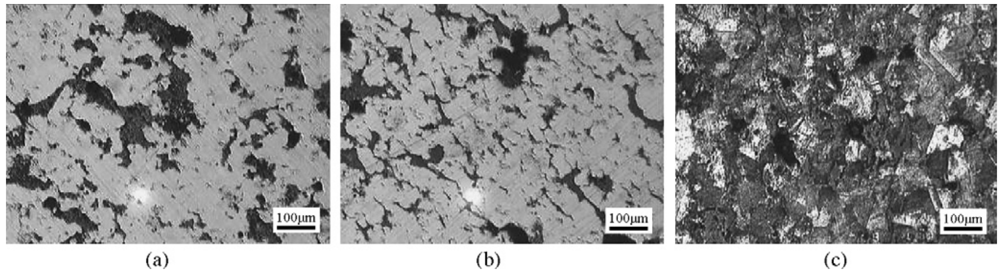

Fig. 3. Micrographs of the test sample. (a) Before metallographic preparation (normal to pressing direction); (b) before metallographic preparation (parallel to pressing direction); (c) after metallographic preparation.

Table 1
Chemical compositions of strip material in mass (wt.%)

Cu	Graphite	Cr	Sn	Pb
80	3.5	3.5	8.5	4.5

Table 2
Properties of contact strip

Density (g/cm^3)	Hardness (HB)	Tensile strength (MPa)	Impact toughness (J/cm^2)
7.4	53	141	4.0

The chemical compositions in mass and mechanical characteristics of the composite materials studied in this paper are shown in Tables 1 and 2, respectively.

2.1.2. Materials

The contact strip was cut into strips of 10 mm × 10 mm × 35 mm to be fit into the sample holder of the wear tester. The counterpart was a band of standard stainless steel 1Cr18Ni9, 50 mm in width and 5 mm in thick.

2.2. Wear test apparatus

The wear test apparatus is shown in Fig. 2. The tester is designed to simulate as closely as possible the relative conditions of the actual tribo-system of a current collector sliding on a stainless steel power rail.

The stainless steel band was wound around a rotary disk, of 405 mm diameter. The wear couples were charged with dc power, with the positive contact on the stainless steel band and the negative on the contact material samples.

The contact material samples are fixed in the insulated specimen holder, which are joined with normal load balance weight.

2.3. Test conditions

All tests were carried out in laboratory environment. The electrical current was set within the contact spot area at the values 0, 10, 20 and 30 A, in according with the maglev vehicle required. The disk was rotated for a cumulative distance of 100 km, at sliding velocities of 25, 50, 75 and 100 km/h. The normal loads of contact were 20 and 40 N in accord with the maglev vehicle's current collector stress in such a small contact spot.

2.4. Inspection

The microstructure of the material was observed under an optical microscope after metallographic preparation. SEM (HITACHI S-2360N) and ESEM (Quanta 200F) equipped with EDS were used for observation of the worn surfaces. Some of the observations were performed without cleaning (in 'as is' condition) in order to observe all the features on the surface including the wear scar and wear debris on the tribo-faces. The wear loss of the test blocks was determined from the weight loss measured by a 1/1000 g high precision electronic digital display microbalance (DT100A).

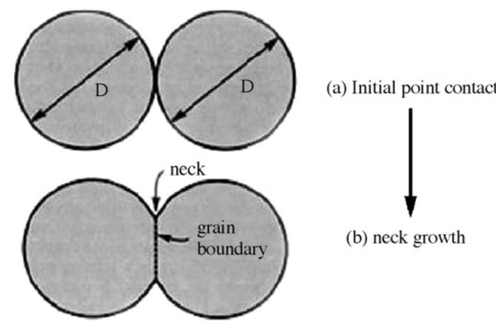

Fig. 4. Two sphere point contact sintering model.

3. Results and discussion

3.1. Microstructure of materials

The microstructure of the test samples, shown in Fig. 3, consists of an irregular copper matrix, with fine graphite powder stored in the pores (the black spots). During the sintering process, the melting copper particles were connected with each other to increase the neck region [2], shown in Fig. 4, and since graphite does not melt with copper, this effect pushed the graphite powder to be stored

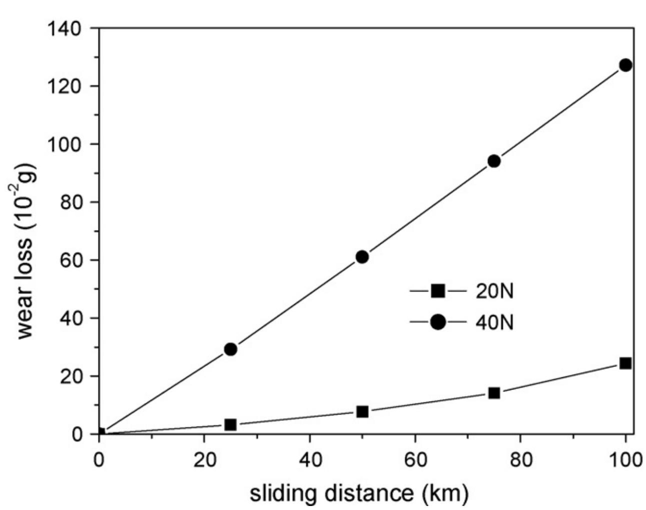

Fig. 5. Effect of load on the wear loss.

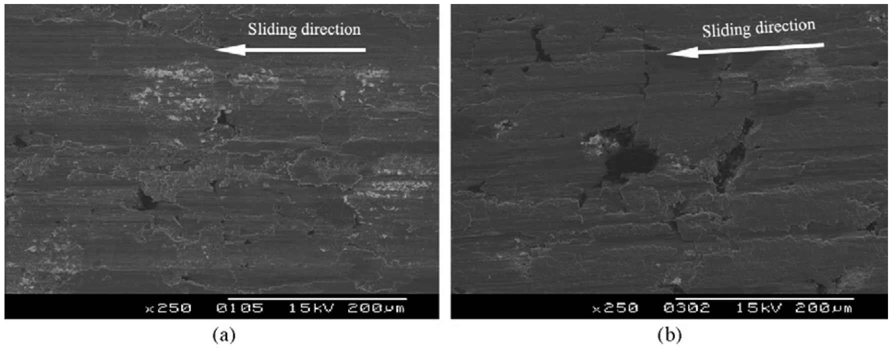

Fig. 6. SEM micrographs of the sample under various loads after 100 km sliding without electrical current. (a) Normal load 20 N; (b) normal load 40 N.

into pores, resulting in a microstructure that resembles nodular casting, but with small pores.

These microstructures have shown the key elements for improving tribological and electrical performance of this material. The copper matrix remains basically unalloyed in the P/M process, thus maintaining its original strength and high conductivity.

3.2. Effect of load, electrical current on the wear rate

Fig. 5 shows the wear loss of the material with sliding distance without electrical current. The tests were performed under applied stress of 20 and 40 N, at a sliding speed of 50 km/h after sliding of cumulative distance 100 km. The results show that the wear loss of the material increases with increasing load.

Fig. 6 shows a number of cracks on the worn surface. The slightly grooved appearance indicates abrasion during sliding. It is noted that the wear loss increased evidently with the increase in normal load. After sliding 100 km, the wear loss under a stress of 40 N is about five times the wear loss under 20 N. In the testing, accumulation of plastic deformation induced by shearing strength can cause numerous cracks on the surface and subsurface, as shown in Fig. 6. Large normal stress can cause increasing shear strength, which is beneficial to plastic deformation. It will cause flake and transfer of material between counter parts. On the other hand, the friction heat produced by the contact stress causes an increase in local surface temperature, which in turn helps to form an oxidation film [12,13], the plasticity of which is sensitive to temperature. The plasticity of the oxidation film reduces rapidly, and the flake will break off when the temperature is over 500 °C [14].

Fig. 7 shows the wear loss of the CGCM with and without electrical current. These tests were performed under an applied normal load of 20 N and at a sliding speed of 25 km/h. The result shows that the wear loss of the material increases with the electrical current.

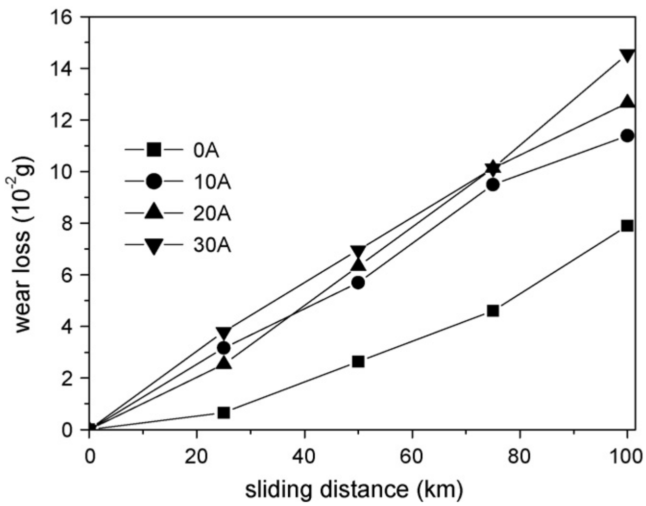

Fig. 7. Effect of current on the friction and wear properties.

Under electrical current, the wear loss almost doubled compared to the cases without electrical current. With electrical current, the total amount of heat produced in wear process comes from three symptoms: electric arc heat, friction heat and Joule heat. The Joule heat originates from the electrical current, as well as from the arc discharge generated between the contact strip and the counterpart stainless steel band when the contact breaks, and makes a significant contribution to the wear loss of the material. The temperature of the arc plasma at the electrode is known to reach 3500–4000 K [1]. The spot of the surface and the subsurface where the arc was discharged increases temperatures promptly. The composite material can melt locally, which results in severe arc erosion.

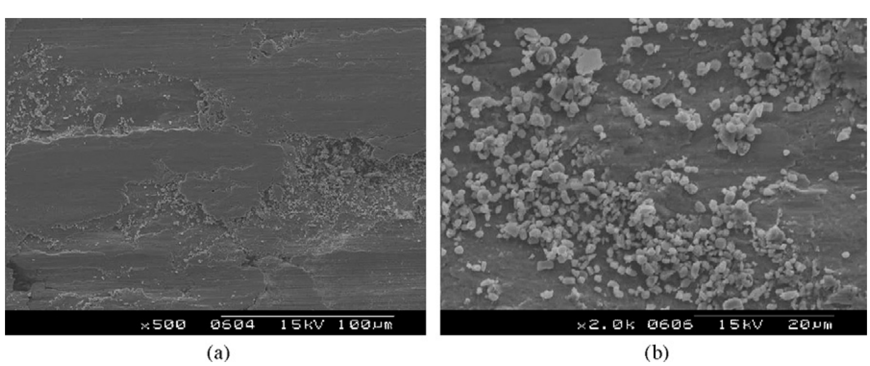

Fig. 8. SEM micrographs of worn surface of the material after 100 km sliding. (a) Worn surface of the material; (b) curved flakes on the worn surface; test condition: 20 N constant normal load, 25 km/h sliding speed, 30 A current.

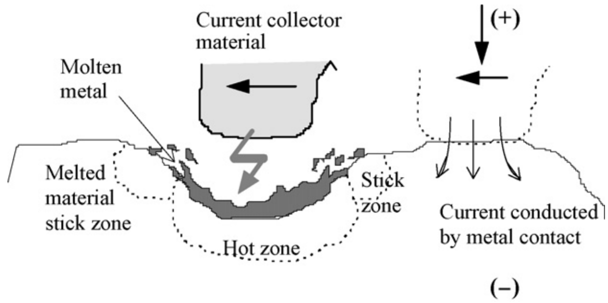

Fig. 9. Schematic model of material loss due to electrical arcing between sliding surfaces.

Fig. 8 shows SEM micrographs of the worn surface of the sample after sliding 100 km under a normal stress of 20 N, at a speed of 25 km/h under a current of 30 A. It is noted that there is much curved flakes debris in the flaking area. In the electrical current wear process, fine grindings were shaved off the surface and were partially melted by the electric arc. Then the semi-molten surface cooled rapidly, causing the particles to adhere to the surface in the flaking areas.

Arcing causes accelerated material loss and is a common appearance when the pantograph or the pole shoe is in abnormal contact with the power rail. An assumed model of this phenomenon is illustrated schematically in Fig. 9.

When an air gap due to the vibration of vehicle, which is defined as momentary separation between two surfaces, occurs in the contact, a discharge of electrical energy occurs in that region, and extensive heat is generated. In the vicinity of that region, material is thought to be vaporized or oxidized by electrical energy discharge and to leave a small pit behind. The wear rate due to electrical discharge has been found to be proportional to the amount of arcing [15]. But it was found that wear with arcing (discharge) is related with the physical properties of counter parts, and the condition of the application. We are still working on the summarization of mathematical formulations, and will be in next paper due to mass content.

3.3. Mechanisms of sliding wear

Several wear mechanisms occur in metal-on-metal sliding situations. These include metal transfer, film formation and removal, debris generation, and cyclic surface deterioration. All of these tribological behaviors depend on the sliding counterparts' characteristics, contact geometry, thermal effects (friction and electric field), chemical environment of the contact, and mechanical parameters of the tribo-system [1].

As shown in Fig. 10(a), graphite and Pb are present as particles in the material. In this form, graphite and Pb can be "smeared" between the counter parts as solid lubricant to improve the wear resistance. It is can be noted that there are numerous nanometer scale Pb particles on the surface, as shown in Fig. 10(b). In an elec-

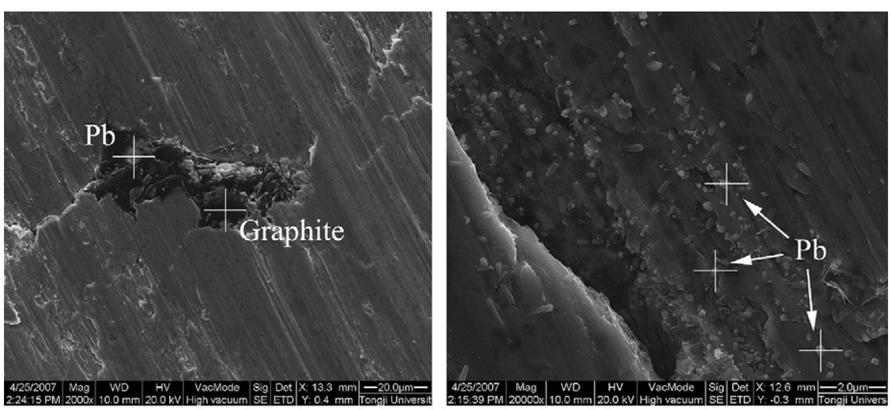

(a) (b)

Fig. 10. Graphite and Pb in the surface after 100 km sliding. (a) Graphite and Pb as particles on worn surface; (b) Pb particles caused by recrystallization; test condition: 20 N constant normal load, 25 km/h sliding speed, 30 A current.

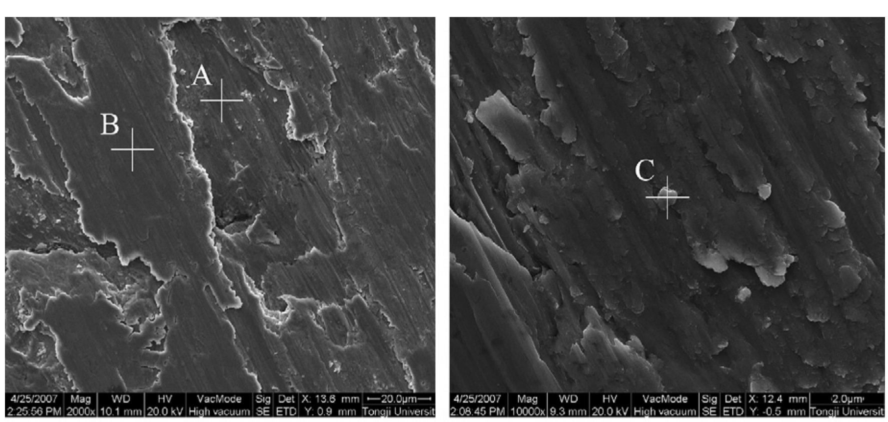

(a) (b)

Fig. 11. Adhesive surface of worn contact strip after 100 km sliding. (a) Different adhesive surface on worn surface; (b) particle contain Fe on worn surface; test condition: 20 N constant normal load, 25 km/h sliding speed, 30 A current.

Table 3
EDS analysis results of worn surface of contact strip, shown in Fig. 111 (wt.%)

Element	Fe	Cu	Cr	Sn	Pb	Si
A	–	83.64	2.67	9.23	4.36	0.11
B	11.48	69.36	5.07	8.55	5.54	–
C	11.12	70.18	4.27	7.89	5.76	0.78

trical wear process, friction heat and electric arc heat can raise the temperature of the surface rapidly. In this process, Pb can be melting, then crystallized to form those particles. It is also noted that the graphite particles stored in the pores of CGCM as the function of self-lubricant, spread over the contact surface without melting during discharging wear.

The EDS analysis results of the worn surface under the electrical current of 30 A at a speed of 25 km/h are listed in Table 3. It shows the presence of graphite and other elements on the worn surface, which indicates the transfer of materials from the stainless steel band to the contact strip due to mechanical and electrical actions during sliding, confirming the adhesive wear mechanism.

It is noted that the thermal effect on interfaces causing softness of contact surface during discharge wear, as the result of wear mechanism has been varied to extend the period of adhesion. CGCM vs. stainless steel is also appeared as low wear rate, compared with the counter parts of CGCM vs. Cu [16] discharging wear rate. There was a very high temperature occurrence causing metal vaporization and oxidization, as the result of loss and cracks of structure. The melting debris spread over the sliding contact materials, and causing the phenomena of metal transferring, therefore, this appearance can be the indication of stick back mechanism. Finally, the wear appeared that the worn contact strip surface was the result of a combined wear mechanism, consisting of adhesion and abrasion. However, such wear counter-part selected in maglev system is preferred as a self-lubricated tribo-system.

4. Conclusions

Based on the laboratory tests, our investigation has led to the following conclusions on the sliding wear behavior of copper–graphite composite material against a stainless steel band.Within the studied range of normal stress and electrical current, the wear loss increased with the increasing normal stress and electrical current.At a sliding speed of 50 km/h after sliding of cumulative distance 100 km without electrical current, the wear loss under a stress of 40 N is about five times to that with 20 N.The wear loss almost doubled under electrical current, compared to the case without electrical current at an applied stress of 20 N at a sliding speed of 25 km/h.Adhesive wear, abrasive wear and electrical erosion wear are the dominant wear mechanisms during the electrical sliding wear processes.

Considering the selection of counterparts for the maglev transportation system, the present work shows that the tribo-system can be improved by the self-lubrication function, and contact materials containing graphite can be implemented into the current collection system.

Acknowledgements

We are grateful to the Program for New Century Excellent Talents of PR China under Grant no. 05-0388, which support this research. We are also grateful to the Center for Materials Testing of Tongji University, where we carried out the test.

This paper was edited by Edit Associates (http://www.edita-ssociates.com).

References

[1] S.G. Jia, P. Liu, F.Z. Ren, et al., Wear behavior of Cu–Ag–Cr alloy wire under electrical sliding, Materials Science and Engineering A 398 (2005) 262–267.
[2] D.H. He, R. Manory, A novel electrical contact material with improved self-lubrication for railway current collectors, Wear 249 (2001) 626–636.
[3] S. Kubo, K. Kato, Effect of arc discharge on wear rate of Cu-impregnated carbon strip in unlubricated sliding against Cu trolley under electric current, Wear 216 (1998) 172–178.
[4] H. Nagasawa, K. Kato, Wear mechanism of copper alloy wire sliding against iron-base strip under electric current, Wear 216 (1998) 179–183.
[5] D.F. Cannon, H. Pradier, Rail rolling contact fatigue research by the European rail research institute, Wear 191 (1996) 1–13.
[6] D.H. He, R. Manory, H. Sinkis, A sliding wear tester for overhead wires and current collectors in light rail systems, Wear 239 (2000) 10–20.
[7] M. Bjordal, E. Bardal, T. Rogne, et al., Erosion and corrosion properties of WC coatings and duplex stainless steel in sand-containing synthetic sea water, Wear 186–187 (1995) 508–514.
[8] H. Zhao, G.C. Barber, J. Liu, Friction and wear in high speed sliding with and without electrical current, Wear 249 (2001) 409–414.
[9] Y. Feng, M. Zhang, Y. Xu, Effect of the electric current on the friction and wear properties of the CNT–Ag–G composites, Carbon 43 (2005) 2685–2692.
[10] A. Bouchoucha, S. Chekroud, D. Paulmier, Influence of the electrical sliding speed on friction and wear processes in an electrical contact copper-stainless steel, Applied Surface Science 223 (2004) 330–342.
[11] S.G. Jia, P. Liu, F.Z. Ren, et al., Sliding wear behavior of copper alloy contact wire against copper-based strip for high-speed electrified railways, Wear 262 (2007) 772–777.
[12] D. Paulmier, A. Bouchoucha, H. Zaidi, Influence of the electrical current on wear in a sliding contact with copper/chrome steel, and connection with the environment, Vacuum 41 (1990) 2213–2216.
[13] A. Bouchoucha, H. Zaidi, E.K. Kadiri, et al., Influence of electric fields on the tribological behaviour of electrodynamical copper/steel contacts, Wear 203–204 (1997) 434–441.
[14] N. Saka, J.J. Pamies-Teixeira, N.P. Suh, Wear of two-phase metals, Wear 44 (1977) 77–86.
[15] O. Oda, Y. Fuji, T. Kohida, Considerations on the arc vanishing time and contactstrip wear of the pantograph connected by means of bus conductor, JSLE Transactions 29 (1984) 463–468.
[16] D.H. He, Test Method of Arcing Behaviour for Railway Current Collection System, WCRR 2001 Köln, Post 300.